Monte Carlo Simulations of Star-Burst Dendrimers

Zheng Yu Chen*

Guelph−Waterloo Program for Graduate Work in Physics and Department of Physics, University of Waterloo, Waterloo, Ontario, Canada N2L 3G1

Shi-Min Cui

Department of Physics, University of Waterloo, Waterloo, Ontario, Canada N2L 3G1

Received September 28, 1995; Revised Manuscript Received September 6, 1996[⊗]

ABSTRACT: Monte Carlo simulations were performed on star-burst dendrimer molecules having various numbers of spacer bonds P and various numbers of generations g. Each molecule is modeled by connecting freely-rotating rigid bonds in a star-burst architecture and by attaching to each end of the bond a hard-sphere bead of diameter d. Dependence of the mean square end−center distance and the mean square monomer−center distance on P, g, and d were each found to follow a power-law scaling behavior in P for fixed g and small d. The results show that the scaling exponent ν for star-burst dendrimers has the same value as that of linear polymers. For different generations g, the asymptotic regime in which the scaling behavior is valid was found to be quite different. In the scaling regime, our results show that the size of dendrimers follows the scaling law $(Pg)^{1-\nu}N^{2\nu-1}$, where N is the total number of monomers in a star-burst molecule. We also discuss physical properties in the high-concentration regime, where the scaling law is no longer valid.

I. Introduction

Star-burst dendrimers are regularly branched polymers synthesized through controlled procedures, generation by generation. At every generation, each external end, which serves as an f-functional branching unit, is connected to an additional $f - 1$ linear portions, each containing P bonds. Recent success in synthesizing dendrimers by using the star-burst approach or the convergent-growth approach has made it possible to experimentally determine the physical properties of these molecules.[1] Theoretical understanding of the conformational properties, however, has not been firmly established.[2−6] The purpose of the present work is to clarify several unanswered questions by means of numerical simulations.

In numerical experiments, polymers in dilute solution in a good solvent have been modeled by various techniques.[7] The model studied here is a molecule of links of N identical rigid bonds of length l, freely joined together in the star-burst formation in D (=3) dimensional space; hard spherical beads of diameter d are attached to the ends of the bonds. As the solvent quality increases, or equivalently the temperature inceases, the star-burst molecules are directly modeled by an increasing bead diameter. The success of the scaling theory for a linear chain in a good solvent is well known; it not only predicts that a universal (i.e., system independent) scaling exponent exists for the polymer size but also produces a scaling parameter through a combination of the excluded volume and the molecular weight.[8,9] The long-wavelength properties of polymers are independent of the microscopic details of the actual interaction potential and only depend on a few physical parameters.[8] Thus for investigating the universal properties of polymers, the freely-joined model suits our purpose.

In this work, we consider the case of trifunctional branching points and *flexible* linear spacers containing P bonds only. The total number of monomers, N, is related to P and the number of generations g by

$$N = 3P(2^g - 1) \tag{1}$$

Thus when g increases, N increases exponentially. It is customary to characterize polymer size by using the mean-square radius of gyration. For star-burst polymers, one may conveniently use the mean-square monomer−center distance, $\langle S^2\rangle$, or the mean-square end-center distance, $\langle R^2\rangle$, as the characteristic size of the molecules, due to the presence of a structural symmetry in the molecules. Throughout this paper, we adopt a system of units such that the length of each rigid bond, l, is set to 1. At the θ point, when the two-body interactions can be ignored, we have effectively $d = 0$; these characteristic sizes, denoted by $\langle S_0{}^2\rangle$ and $\langle R_0{}^2\rangle$, respectively, may be calculated analytically,

$$\langle R_0{}^2\rangle = Pg \tag{2a}$$

and

$$\langle S_0{}^2\rangle = \frac{N}{N+1}\left[\frac{1}{2} + P\left(g - \frac{3}{2}\right) + \frac{Pg}{2^g - 1}\right] \tag{2b}$$

Equation 2a is simply the mean-square end-to-end distance of a random walk of total step length Pg, for a single branch extending from the center to the external end.

For convenience, we also use the notation $S = \langle S^2\rangle^{1/2}$, $S_0 = \langle S_0{}^2\rangle,^{1/2}$ $R = \langle R^2\rangle^{1/2}$, and $R_0 = \langle R_0{}^2\rangle^{1/2}$ below. When repulsive interactions between the monomers are present, the molecules begin to swell. In the scaling regime, the asymptotic behavior for large P is expected to follow a power law behavior $S^2 \propto P^{2\nu}$, where ν is the critical exponent; a g-dependent coefficient may exist in this expression. In the theory of linear polymers with a large length P,[10] it is well-known that the asymptotic scaling behavior can be described by specifying by a parameter z, defined as $z = uP^{(4-D)/2}$, where $D = 3$ is the dimensionality of the system and u is the interaction constant. A naive guess would be to define a scaling parameter for star-burst molecules in a similar way. In this paper, we assume that we may define a similar z which is proportional to $P^{(4-D)/2}$ in the large-P limit and

[⊗] Abstract published in *Advance ACS Abstracts,* October 15, 1996.

S0024-9297(95)01463-X CCC: $12.00

which contains a g-dependent factor:

$$z = uN{S_0}^{2-D} \tag{3}$$

We can then conveniently write

$$S^2/{S_0}^2 = A(g)z^{2(2\nu-1)/(4-D)} \tag{4}$$

In general, the coefficient $A(g)$ depends on g but approaches a constant for large g as demonstrated by our simulation data presented below. In terms of the Flory exponent $\nu = {}^3/_5$ for a $D = 3$ system, eqs 3 and 4 imply simply that $S \propto (Pg)^{2/5}(uN)^{1/5}$ for large g.

Although the statistics of branched polymers had already been discussed by Zimm and Stockmayer as early as 1949,[11] the conformational properties of dendrimers in good solvents were not examined using scaling concepts until much later. A self-consistent field theory,[2] based on a stretched-spacer assumption where u is assumed to have the magnitude l^3, yields various statistical properties of dendrimers. Lescanec and Muthukumar,[3] who were interested in scaling behavior in the low-volume concentration regime, performed computer simulations by implementing a kinetic-growth algorithm. With a fixed excluded-volume diameter to bond length ratio ($d/l = 1/1.2$), they considered the cases of $P = 1$, 3, 5, 7, 9, and 11 with g ranging from 1 to the corresponding maximum growth generations. Most of their systems actually lie in the moderate-concentration regime and their results showed qualitative differences from those predicted by the de Gennes−Hervet model. However, the use of the kinetic-growth algorithm is questionable since it lacks a relaxation mechanism allowing the systems to reach equilibrium. Following Lescanec and Muthukumar's idea, Mansfield and Klushin further generalized the algorithm to estimate the intrinsic viscosity.[4] In a subsequent paper,[5] Mansfield and Klushin explored the conformational properties of dendrimers by using a Monte Carlo (MC) simulation on a diamond lattice with fixed spacer length ($P = 7$). Their results were expressed in terms of varying g while d^2 and P are fixed. Their density profiles resemble those found in this work.

In this paper, we present an MC simulation of the freely-joined model mentioned above for $g = 1$, 2, 3, ..., 7 with P varying from 1 to the maximum value allowed by the limitation of our computer. For each set of g and P, several values of the excluded-volume diameter d are considered. Our results give a complete physical picture which extends from the scaling regime to the high-concentration regime. The simulation method used here also avoids the potential pitfalls of the kinetic-growth model.

The dependence of their physical properties on g makes the problem of dendrimers more complicated than that of linear polymers. We shall address this problem below by examining several aspects that interest us here. First, *given that there could be a g-dependent coefficient*, we would like to confirm the prediction that the scaling exponent ν has the linear-chain value. According to the model of de Gennes and Hervet,[2] by ignoring the g factor in their expression, the scaling exponent ν should have the value $\nu = 0.6$, in agreement with the linear-chain exponent of Flory.[12] Later, it was shown quite generally by Duplantier, based on a renormalization calculation, that ν of regularly branched polymers has the linear-chain value.[13] The ϵ-expansion of ν by Biswas and Cherayil directly demonstrated that ν for dendrimers has the same expression as ν for linear chains up to order ϵ.[6] Note that $\nu = 0.6$ is not too different from the "true" value $\nu = 0.589$ for linear chains,[10] the latter being the critical exponent observed in the present work. This evidence overwhelmingly supports the conclusion that the molecular size of dendrimers should scale according to the linear-chain exponent in P. The kinetic-growth model,[3] however, showed a mean-square radius of gyration data obeying the scaling law $\langle R_g^2\rangle \propto N^{0.44\pm0.04}P$. By ignoring the g dependence once again, this scaling law predicts a scaling exponent $\nu = 0.72 \pm 0.02$, which is much larger than the linear-polymer value. This scaling law, however, was determined from simulation data at moderate to high monomer densities; as such, it is invalid in the low-density regime where the conventional exponent ν is defined. As demonstrated below, correction-to-scaling terms may become important and severely affect the determination of the critical exponent for d/l as large as 0.83, which is the ratio used by Lescanec and Muthukumar. It is this reason, together with the previously stated problem of using the kinetic-growth algorithm, that leads to an overestimation of ν by these authors. Whether there is a different power law that the high-density data would follow is a separate issue.

Next, unlike the scaling behavior in P, upon which most theories agree, the particular functional dependence of the molecular size on g is not clearly understood. Different theories give different results. The self-consistent model[2] predicted that $R^2 \propto N^{0.4}P^{0.8}$. Because the self-consistent theory is based on the stretched-spacer assumption, which has been shown to be problematic in describing dendrimer structures,[3,5] the correctness of the g dependence resulting from this model is rather doubtful. The kinetic-growth model[3] suggested that $\langle R_g^2\rangle \propto N^{0.44\pm0.04}P$; besides the problems associated with the adoption of the kinetic-growth model, this result could be, again, affected by nonuniversal behaviors. Perturbation theory does give an expression for the g dependence in question,[6] but it is quite complicated and it is only correct perturbatively. Using the definitions in eqs 3 and 4, our simulation data show that $A(g)$ approaches a constant at large g, indicating an asymptotic behavior $S^2 \propto (Pg)^{2(1-\nu)}(uN)^{2(2\nu-1)}$.

A related problem is the size of the scaling regime. To correctly obtain scaling behavior, it is important to analyze the numerical or experimental data inside the scaling regime. According to our data, a basic criterion, subject to the further restriction that P must be large, is that the volume density must be smaller than 0.04 for the power-law behavior to be valid with a relative error less than 10%. The scaling regime then lies in the low volume density regime. Since the total number of monomers in a dendrimer increases exponentially as a function of g, the size of the scaling regime decreases drastically when g increases. Most experimental and simulation data for large g and large excluded volume fall in the nonscaling regime. Therefore, carrying out a simple power-law fitting outside the scaling regime will probably result in erroneous conclusions. Our analysis was carefully conducted so that the different regimes were compared.

The most radical difference between the structures of star-burst molecules and conventional linear polymers is the structural constraint on the star-burst molecules that makes them much denser than the latter. The existence of a critical generation, g_c, beyond which the molecules cannot grow further, was first

discussed theoretically by de Gennes and Hervet,[2] who estimated g_c based on balancing forces at the branching points using a self-consistent method. In the high-density region when g is just below g_c, they predicted that the molecules become highly, if not completely, stretched, characterized by a maximum in the concentration distribution near the outmost edge of the molecule, and by a mean-square end−center distance which roughly scales as $S \propto P$. One of the current controversies is whether such a "hollow" distribution indeed exists.[1] We will examine a few special cases in the concentrated regime. Due to the limitation of our data, we are not able to give a complete physical picture of the high-volume concentration regime.

This paper is organized as follows. In section II we introduce the model and the numerical procedure in detail and define the physical quantities evaluated in the numerical experiment. In section III we present a discussion of the results, and compare them with results from other models. Section IV is a brief summary.

II. Model and Simulation Method

There are several techniques that one may adopt for the simulation procedure. The Monte Carlo method used in this study is a generalization of the off-lattice pivot method developed for linear chains and randomly branched polymers.[14] At each MC step, a bead was chosen at random from the N beads in the molecule, and the nearest-neighbor bead that is closer in path distance to the center was identified and used as the rotation center. Monomers that were rooted from the chosen bead were rotated in space about the rotation center as a rigid body by specifying random values for the three Euler angles. Note that the Euler angle associated with the rotation of the z axis must be chosen so that the cosine of this angle is evenly distributed between $[-1,1]$. Each new position of the rotated monomers was checked by a volume-excluding subroutine; if the new position overlaps with the excluded-volume region of the monomers on the unrotated part of the polymer, the attempt was considered failed and a new MC step was considered.

For a given set of parameters, an initial configuration was generated by using a kinetic method similar to that of Lescanec and Muthukumar.[3] The whole molecule was grown from a central core, generation by generation. Each new position was checked; if placing a bead would overlap with any existing monomers, attempts were made to find an alternative position that did not have this problem. After a maximum of 1000 attempts, we would always accept the position. This way, we might generate a preliminary configuration with a minimum number of overlapping monomers. This preliminary configuration was then regarded as a nonequilibrium state and was allowed to relax to a nonoverlapping state by using a special numerical method that always looks for a smaller number of overlapping monomers. During the process of generating the initial configurations, we noticed that the molecules produced this way were always much smaller in size compared to their equilibrium counterparts. This already indicates a potential problem with the kinetic method for estimating the molecular size.

After removing overlapping of the monomers, the systems were then allowed to further relax to an equilibrium state. The numbers of MC steps that were used for this purpose typically ranged from 10^4 for small molecules to 10^5 for large molecules. For especially

Table 1. MC Simulation Data for the Mean-Square Monomer−Center Distance

g	P	$\langle S^2\rangle/\langle S_0^2\rangle$			
		$d^2 = 0.125$	$d^2 = 0.250$	$d^2 = 0.500$	$d^2 = 0.990$
1	2	1.028	1.064	1.124	1.211
	4	1.083	1.175	1.333	1.531
	8	1.156	1.349	1.613	1.959
	16	1.247	1.529	1.935	2.446
	32	1.373	1.769	2.306	3.006
	64	1.483	2.006	2.724	3.545
	128	1.650	2.318	3.125	4.183
	256	1.833	2.581	3.614	4.841
	512	2.047	2.986	4.100	5.614
	1024	2.316	3.314	4.735	6.473
	2048	2.557	3.804	5.319	7.219
		$d^2 = 0.100$	$d^2 = 0.200$	$d^2 = 0.400$	$d^2 = 0.990$
2	1	1.029	1.059	1.125	1.234
	2	1.071	1.182	1.357	1.596
	4	1.150	1.338	1.626	2.059
	8	1.243	1.526	1.932	2.592
	16	1.370	1.724	2.256	3.196
	32	1.473	1.943	2.673	3.840
	64	1.638	2.182	3.051	4.488
	128	1.783	2.489	3.536	5.313
	256	2.025	2.867	4.077	5.985
	512	2.224	3.157	4.552	6.973
	1024	2.445	3.570	5.090	7.860
		$d^2 = 0.100$	$d^2 = 0.200$	$d^2 = 0.500$	$d^2 = 0.990$
3	1	1.065	1.149	1.328	1.474
	2	1.152	1.326	1.657	1.925
	4	1.258	1.528	2.033	2.497
	8	1.391	1.750	2.481	3.149
	16	1.541	1.982	2.939	3.790
	32	1.645	2.254	3.403	4.483
	64	1.864	2.526	3.979	5.318
	128	2.060	2.934	4.514	6.101
	256	2.294	3.253	5.106	6.937
	512	2.601	3.750	6.015	7.879
		$d^2 = 0.100$	$d^2 = 0.150$	$d^2 = 0.500$	$d^2 = 0.990$
4	1	1.138	1.200	1.551	1.741
	2	1.265	1.399	1.932	2.318
	4	1.414	1.605	2.419	2.912
	8	1.589	1.798	2.843	3.695
	16	1.749	2.030	3.408	4.475
	32	1.947	2.318	3.926	5.370
	64	2.135	2.574	4.498	6.199
	128	2.394	2.933	5.286	7.125
	256	2.669	3.270	6.104	8.177
		$d^2 = 0.050$	$d^2 = 0.130$	$d^2 = 0.500$	$d^2 = 0.990$
5	1	1.109	1.309	1.814	2.096
	2	1.209	1.547	2.373	2.786
	4	1.341	1.760	2.830	3.557
	8	1.456	2.073	3.453	4.260
	16	1.554	2.260	4.018	5.404
	32	1.710	2.633	4.771	6.373
	64	1.851	2.834	5.578	6.906
	128	2.153	3.311	6.394	8.461
		$d^2 = 0.040$	$d^2 = 0.100$	$d^2 = 0.200$	$d^2 = 0.990$
6	1	1.170	1.418	1.726	2.446
	2	1.328	1.712	2.110	3.341
	4	1.459	1.959	2.571	4.376
	8	1.610	2.246	3.012	5.402
	16	1.763	2.456	3.418	6.476
	32	1.959	2.793	3.832	7.724
	64	2.162	3.185	4.435	8.481
		$d^2 = 0.020$	$d^2 = 0.075$	$d^2 = 0.200$	$d^2 = 0.990$
7	1	1.156	1.537	2.004	2.897
	2	1.309	1.946	2.606	3.579
	4	1.427	2.162	3.179	4.549
	8	1.555	2.525	3.694	5.687
	16	1.769	2.764	3.987	7.236
	32	1.938	3.181	5.113	8.877
8	2				4.705
9	2				5.591

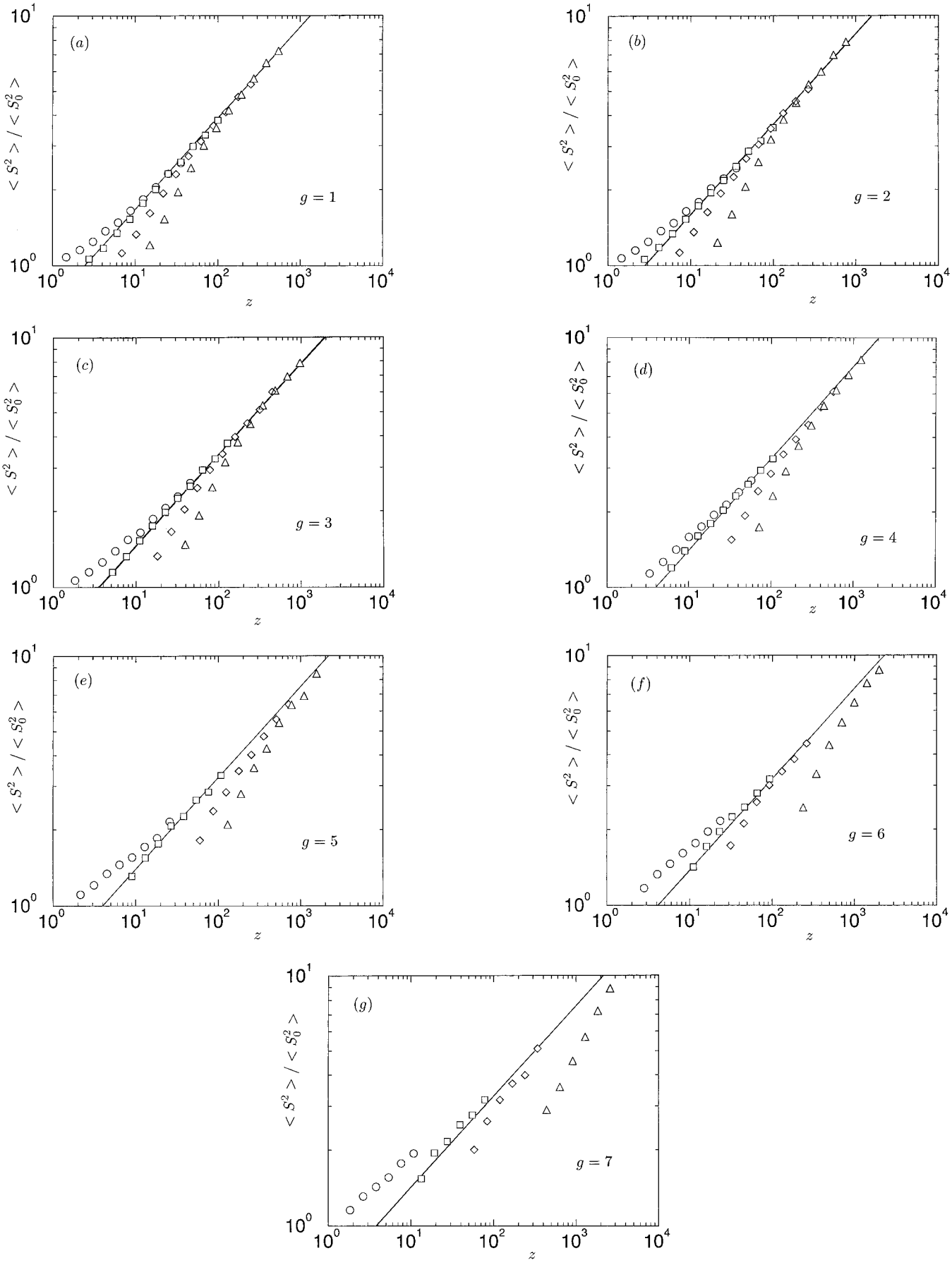

Figure 1. Scaled mean-square monomer−center distance $\langle S^2 \rangle$ as a function of z defined in eq 3 for $g = 1$, 2, 3, 4, 5, 6, and 7. Here, the scaling factor $\langle S_0^2 \rangle$ is defined in eq 2b. The circles represent the data points in the third column of Table 1, squares the fourth, diamonds the fifth, and triangles the sixth. The solid straight lines represent power laws with an exponent equal to $2(2\nu - 1) = 0.356$, with amplitudes listed in Table 2; see eq 4.

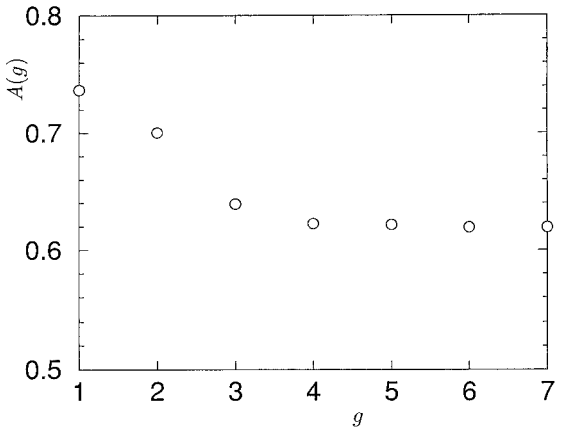

Figure 2. Coefficient $A(g)$ as a function of g.

Table 2. $A(g)$ and $u^*(g)$ Estimated from Figure 1 for Different g

g	$A(g)$	$u^*(g)$
1	0.737 ± 0.002	0.524 ± 0.02
2	0.700 ± 0.002	0.375 ± 0.04
3	0.639 ± 0.004	0.375 ± 0.06
4	0.623 ± 0.004	0.243 ± 0.04
5	0.622 ± 0.010	0.196 ± 0.02
6	0.619 ± 0.020	0.132 ± 0.02
7	0.623 ± 0.030	0.086 ± 0.02

large and dense systems, as many as 3×10^6 MC steps were used for equilibration. Upon reaching equilibration, various configurations of the systems were simulated by using the nonlocal pivot algorithm described above. A typical run consisted of 2×10^5 to 2×10^6 MC steps; the structure was analyzed and the structural data were collected every 5 MC steps. In general, the average acceptance rate ranged from approximately 0.18 for large d to 0.8 for small d. We considered the cases $g = 1$, 2, 3, 4, 5, 6, and 7 and $P = 1$, 2, 4, 8,.... The maximum value of P was determined by the restriction that the total number of monomers N would not exceed 1.3×10^4. Otherwise, it would be computationally too costly. For each set of g and P, several values of d were considered.

We treated all monomers as having an equal molecular weight. In our notation, the central core is labeled $\mathbf{R}_0$, and the position vector of the ith monomer is labeled $\mathbf{R}_i$. Table 1 is a summary of the simulation data for the mean-square monomer−center distance S^2, where S^2 is defined as

$$S^2 = \frac{1}{N+1}\sum_{i=0}^{N}\langle(\mathbf{R}_i - \mathbf{R}_0)^2\rangle \tag{5}$$

We also recorded data for the mean-square end-center distance R^2, where R^2 is defined as

$$R^2 = \frac{1}{K}\sum_{i=1}^{K}\langle(\mathbf{R'}_i - \mathbf{R}_0)^2\rangle \tag{6}$$

Here, $K = 3{\cdot}2^{g-1}$ is the total number of external ends, and $\mathbf{R'}_i$ is the position vector of the ith external end. We found that the data for R and S display exactly the same behavior, and thus we shall only discuss the properties of S in this paper. We also collected information on the monomer distribution which will be discussed in the next section.

The pivot algorithm was shown by Madras and Sokal for a lattice implementation[14] to statisfy the requirement of detailed balance. To further verify its validity, we also adopted a generalized kink-jump method to calculate the conformational properties for several sets of (P,g). This method generates highly correlated new configurations and thus needs many more MC steps to calculate every data point. The results from both calculations agreed with each other within the estimated errors.

III. Discussion

One of the advantages of the off-lattice method is its flexibility in controlling the diameter of the beads d and thus the averaged excluded volume per bond u. The definition of u based on d, however, is not quite so straightforward. Here we use the following simple argument to calculate u.[15] Consider a single bond of length $l = 1$ that is associated with two beads at each end. If $d < {}^1/_2$, the region excluded per bond by these two beads when a third bead is introduced is simply the volume of two separate half-spheres of radius d. On the other hand, if $d \geq {}^1/_2$, indicating these half-spheres sharing a common region, then the actual excluded region felt by the third bead is the volume of the two half-spheres of radius d minus the volume of the overlapping region. Thus

$$u = {}^4/_3\pi d^3, \qquad d < {}^1/_2 \tag{7a}$$

$$u = \pi[d^2 - {}^1/_{12}], \qquad d \geq {}^1/_2 \tag{7b}$$

Note that this formula has been successfully used to analyze the conformational properties of linear polymers[16] and *randomly* branched polymers.[17]

Figure 1 displays the quantity $\langle S^2\rangle/\langle S_0{}^2\rangle$ as a function of the scaling parameter z defined in eq 3 for $g = 1$, 2, 3, 4, 5, 6, and 7. The conventional way to analyze such MC data is to fit it to a power law in order to determine the appropriate exponent. Fitting in this way often results in an effective exponent rather than the real one. As shown by the plots in Figure 1, analyzing any particular set of data for a given set of (d,g) will yield rather different values for the effective exponent. Here we examine the problem from a different perspective.

The essential difficulty encountered in analyzing such data is due to the strong correction-to-scaling behavior of various d.[18,19] By visually inspecting the plots in Figure 1, we may easily conclude that a scaling regime indeed exists for large z. The question then becomes, given that the scaling exponent ν is the same as that for a linear chain (for which a very accurate estimation exists[10]), can we satisfactorily explain other interesting features of these data? We plot straight lines in Figure 1 in order to demonstrate the power law with a scaling exponent having the linear-chain value:[10] $\nu = 0.589$. The lines are manually produced by carefully moving the straight lines to the appropriate places while keeping the slope equal to $2(2\nu - 1) = 0.356$, so that the data points seem to approach the straight line asymptotically at large z. All seven plots show that the asymptotic behavior corresponding to various d can indeed be accounted for by the straight lines, and this indicates that the conformational properties of star-burst molecules belong to the same universality class as linear chains. Our choice of ν is justified by previous theoretical[6,13] results. As a special case of $g = 1$, the molecular size of star polymers scales according to the linear-chain exponent.[6,20,21]

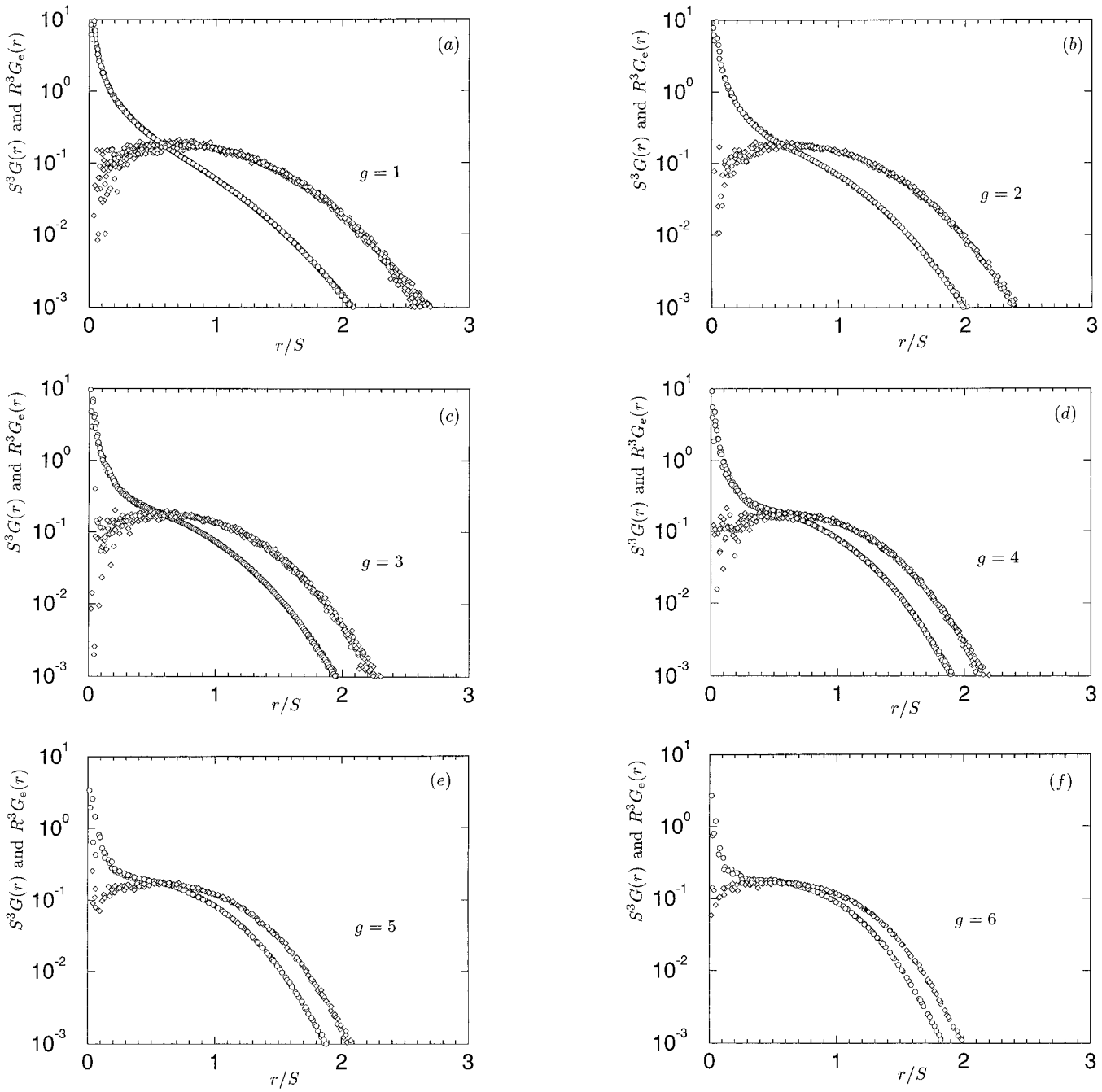

Figure 3. Scaled monomer distribution $S^3G(r)$, represented by the circles, and scaled end-monomer distribution $R^3G_e(r)$, represented by the diamonds, for various values of g. The curves are plotted by using the distribution data of the systems that produce S obeying the scaling law, recorded during the simulation. Different sets of P, g, and d^2 are considered. Note a weak minimum exists at the center of the $R^3G_e(r)$ function.

Based on the above analysis, we were able to estimate the g-dependent coefficient $A(g)$ in eq 4, which is listed in Table 2. For various g, the errors were estimated according to the confidence of placing the straight lines in the corresponding plot in Figure 1. Looking at the asymptotic behavior of $A(g)$ in the large-g limit strongly suggests that $A(g)$ approaches a constant $A(g \gg 1) = 0.62 \pm 0.03$ (see also Figure 2). Alternatively, the existence of a constant $A(g)$ in the large-g limit indicates that we have chosen the correct g-dependent factor in z. As discussed in the Introduction, the scaling dependence on g has not been satisfactorily explained by existing theories.

The field theory approach to the conformational properties of polymers asserts that the excluded-volume parameter u plays the same role as the coupling constant in a ϕ^4 theory for a critical magnetic spin system.[8] Renormalization group theory states that, in principle, there exists a Wilson fixed point when u has a special value u^* such that the scaling behavior in eq 4 is valid without the correction-to-scaling terms. Otherwise for arbitrary u, the expression must be amended as[22,23]

$$S^2/{S_0}^2 = A(g)z^{2(2\nu-1)}[1 + B(1 - u/u^*)z^{-2\Delta} + ...] \quad (8)$$

where B is a constant that probably depends on g in our case. The correction-to-scaling exponent Δ was estimated to be $\Delta = 0.46$ for linear chains. Note how the coefficient of the $z^{-2\Delta}$ term depends on u. Since $B > 0$, the sign of the coefficient is directly related to the

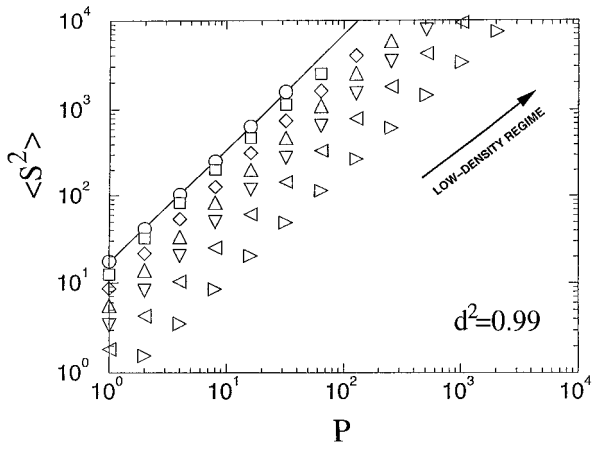

Figure 4. Mean-square center−monomer distance as a function of P for various g at $d^2 = 0.99$. Most data points are in the high volume density regime. Starting from the bottom, $g = 1$ (right triangles), $g = 2$ (left triangles), $g = 3$ (down triangles), $g = 4$ (up triangles), $g = 5$ (diamonds), $g = 6$ (squares), and $g = 7$ (circles).

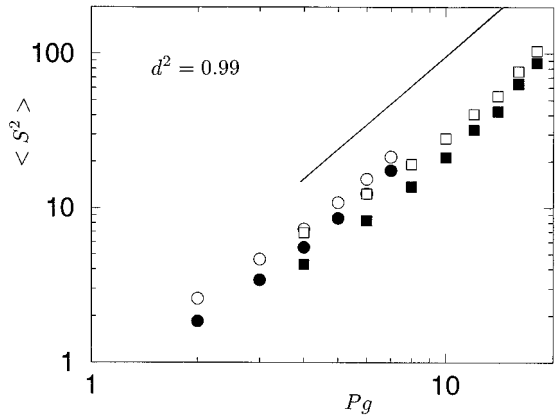

Figure 5. Molecular size of dendrimers as a function of Pg for $P = 1$ (circles) and $P = 2$ (squares), with $d^2 = 0.99$. The open and closed symbols represent R^2 and S^2, respectively. The $P = 1$ case corresponds to the Cayley tree model. A straight line is plotted to show the asymptotic behavior $\langle S^2 \rangle \propto g^2 l^2$ for large g, to which the $P = 1$ data points are seen to follow. The critical generations are estimated to be $g_c(P=1) = 8$, and $g_c(P=2) = 10$.

sign of $(1 - u/u^*)$. Therefore, the $u > u^*$ and $u < u^*$ curves have opposite curvatures in the log−log plot. Nickel noted that these u-dependent behaviors give rise to system-dependent corrections to scaling for the case of linear chains,[18] for which u^* should have a value slightly smaller than l^3.[18,24] As a consequence, the self-avoiding-walk data on lattices, corresponding to $u > u^*$, always show a negative correction to scaling;[18,24] the off-lattice data for various values of u shows both correction behaviors depending on the size of u.[16] Our situation here is quite similar to the off-lattice data of linear chains.

Although the situation may be further complicated by three-body interactions and by high-order correction-to-scaling terms, we assume here that the linear correction term in eq 8 dominates. This leads us to an estimate for u^*, corresponding to the fixed-point value of the bare coupling constant, based on the plots in Figure 1. We have simply taken the value of u corresponding to which the deviations from a straight line are a minimum. Table 2 is a list of the $u^*(g)$ obtained this way. The data indicate that $u^*(g)$ has a strong g dependence. Due to the large uncertainty in these estimates, it is difficult to give a more quantitative analysis.

For those systems whose S lie in the scaling regime, the monomer distribution as a function of r should also exhibit scaling behavior. We selected a few representative systems for each g and plotted the scaled monomer distributions, $S^3G(r)$, and the scaled distributions of the end monomers, $R^3G_e(r)$, as functions of r/S in Figure 3. Here $G(r)$ (or $G_e(r)$) was determined in the simulation as the probability of a monomer (or an end monomer) appearing in a unit volume at a distance r from the center. In producing these figures, we have removed the strong peak at $r = 0$ due to the permanent presence of the center monomer. It is interesting to observe that the monomer distribution $G(r)$ displays a maximum at the center, as observed previously by Lescanec and Muthukumar,[3] and that the end-monomer distribution $G_e(r)$ displays a weak maximum near the edge of the molecule. The depletion of the distribution function $G_e(r)$ at the center indicates that, even for dilute solutions, the end monomers prefer to stay away from the central core region. At the same time, there is no physical reason for the end-monomer distribution to display the type of hollow core discussed in ref 2; there the depletion is probably produced by the rather artificial assumption of a stretched-spacer model, and that would simultaneously produce a hollow-core monomer distribution, not clearly observed in our model.

The distribution functions for $g = 4$, 5, and 6 in Figure 3d−f collapse into a universal curve. Just as the numerical data for $A(g)$ show, the large-g limit is reached in only a few generations.

It is imporatnt to note that the increasing segment volume fraction due to an increasing g is responsible for moving the system away from the scaling regime. For large g at a fixed u, the size of a dendrimer departs significantly from the scaling behavior described in eq 4. The data points in Figure 1 for $d^2 = 0.99$ (triangles in all the plots) demonstrate the increasing importance of the nonuniversal behavior when g increases. The asymptotic region can only be reached when z is asymptotically large. Since the scaling regime becomes very small for large g, any experimental attempt to examine the scaling behavior of a large-g system should be performed very close to the Θ point (to get a small u/u^*) with very large N (to get a large z). The same caution must be taken when analyzing data from the MC simulations; this is a point which is not always carefully appreciated when numerical experiments are performed.

A systematic method for estimating the size of the scaling regime should invoke a criterion based on the comparative magnitudes of the correction-to-scaling term and the scaling term in eq 8. Since we do not have a reliable estimate of $B(g)$, here we consider the average volume density estimated by $\rho = (d/2)^3 N/S^3$. Our data show that, in general, all the data points corresponding to $\rho > 0.04$ have a deviation of 10% or more from the scaling behavior, for various values of g, P, and d^2. Thus the scaling regime corresponds to systems of low volume densities. Systems having $\rho < 0.04$, however, do not necessarily display the asymptotic scaling behavior. An additional restriction is to have a large P, a condition that must be considered even in the case of linear chains.

In the preceding analysis, we have mainly focused on the scaling regime where the monomer volume concentration is generally low. We consider now a series of systems for a given d^2 (=0.99) at high monomer volume

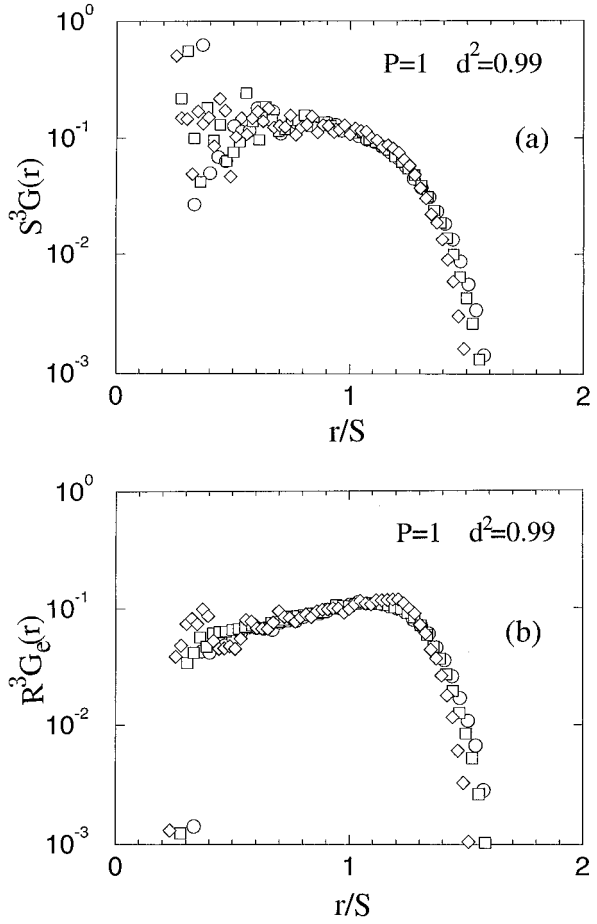

Figure 6. (a) Scaled monomer distribution $S^3G(r)$ and (b) scaled end-monomer distribution $R^3G_e(r)$ for $P = 1$, $d^2 = 0.99$, and $g = 5$ (circles), 6 (squares), and 7 (diamonds). The fine structure of the oscillation of the data points near the center is plotted in Figure 8.

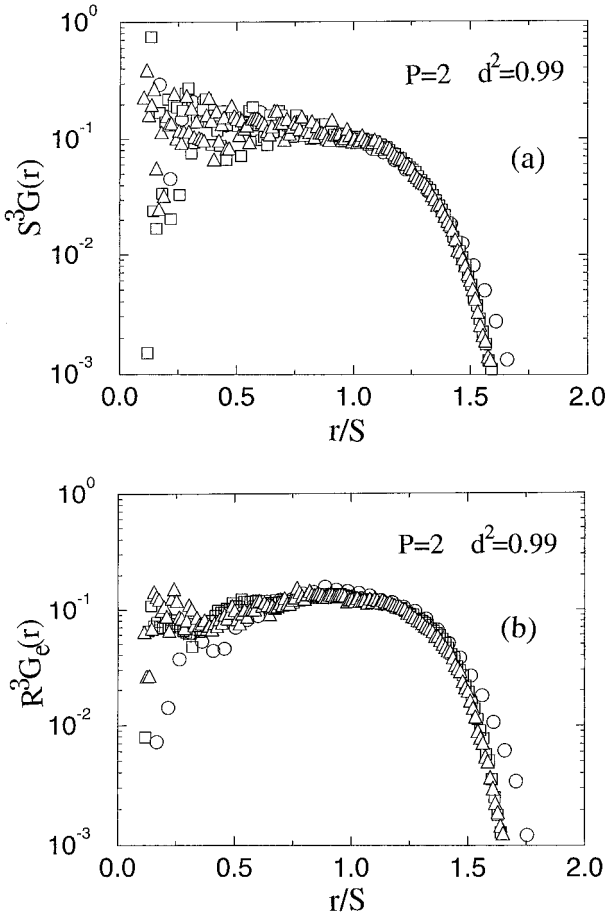

Figure 7. (a) Scaled monomer distribution $S^3G(r)$ and (b) scaled end-monomer distribution $R^3G_e(r)$ for $P = 2$, $d^2 = 0.99$, and $g = 7$ (circles), 8 (squares), and 9 (triangles). The fine structure of the oscillation of the data points near the center is plotted in Figure 9.

concentrations. In Figure 4, the mean-square monomer−center distance S^2 is plotted as a function of P, where the different symbols correspond to different values of g. The data points near the upper left corner correspond to systems with relatively high monomer density. It is interesting to observe that S^2 corresponding to $g = 7$, represented by circles in Figure 4, effectively follows a power-law $S^2 \propto P^{1.30}$, which also seems to be the asymptotic behavior for all other g's at smaller P. The crossover to the power-law behavior $S^2 \propto P^{1.178}$ takes place at much larger P as shown in Figure 1.

A different perspective is gained by observing systems with a constant d^2 (=0.99) and at fixed P, with varying g. De Gennes and Hervet[2] showed that there exists a critical generation g_c giving an upper limit for the possible number of generations, and they concluded that $g_c \propto 2.88 \ln P + 4.4$. During the preparation of our initial configurations, we determined the critical generations $g_c \approx 8$, 10, and 11 respectively for $P = 1$, 2, and 3, by using the criterion that g_c corresponds to the number of generation at which the preliminary configuration produced with overlapping monomers can no longer relax to a nonoverlapping equilibrium state. The approach to g_c was also accompanied by a dramatic reduction in the MC acceptance rate, indicating a drastically increasing volume concentration. We do not have enough data points for g_c to quantitatively compare to the de Gennes−Hervet critical generation estimate. On the other hand, Lescanec and Muthukumar[3] found that kinetic self-avoiding walks stop at an average generation $g_c(P=1) \approx 5.8$ and $g_c(P=2) \approx 6.1$, even though the volume concentration of the systems considered in their model is generally lower than ours due to smaller monomers ($d = 1/1.2$). In reality, the limiting growth of dendrimers may likely follow a de Gennes−Hervet-type logarithmic law.

When g increases for fixed values of d and P, the system becomes denser and denser; the new monomers always seek new space beyond the highly packed core region that is already occupied by existing monomers. Then, we may speak of a highly stretched structure for g close to g_c. The open and closed circles in Figure 5 represent S^2 and R^2 as functions of g for $P = 1$ (Cayley tree). These quantities are seen to approach an asymptotic behavior

$$S, R \propto gl \tag{9}$$

near g_c, which agrees well with the above qualitative physical picture. The question now arises: how would the molecular size for other values of P behave near g_c? Interestingly, the molecular size for $P = 2$ grows faster when g increasses, following a power law faster than that given by eq 9, which is a behavior that cannot be simply explained by the use of the stretched-spacer picture (see the squares in Figure 5).

In the high volume concentration regime, it is generally speculated that the monomer distribution will show a depletion at the center (the hollow-core model). The scaled distribution functions displayed in Figures 6 and 7 for $P = 1$ and $P = 2$, however, only clearly indicate a

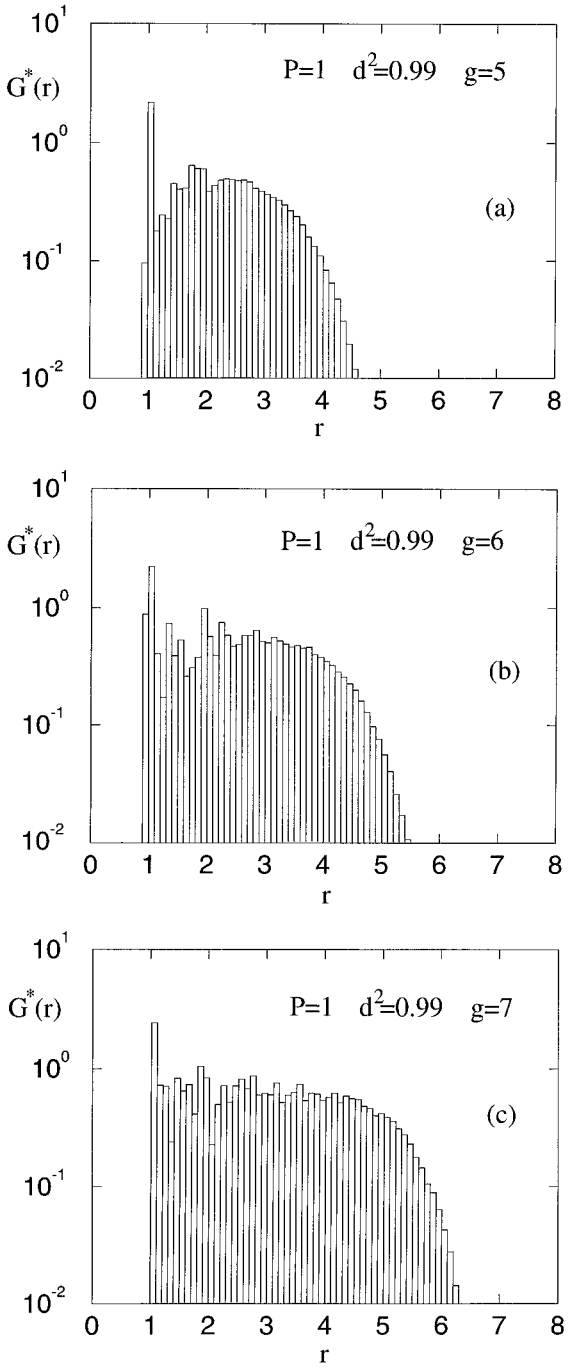

Figure 8. Monomer density as a function of the distance from the center for $P = 1$, $d^2 = 0.99$, and various g as specified in the figures. The strong peaks near $r = 1$ are due to the three beads connected to the center. These systems are in the high volume density regime.

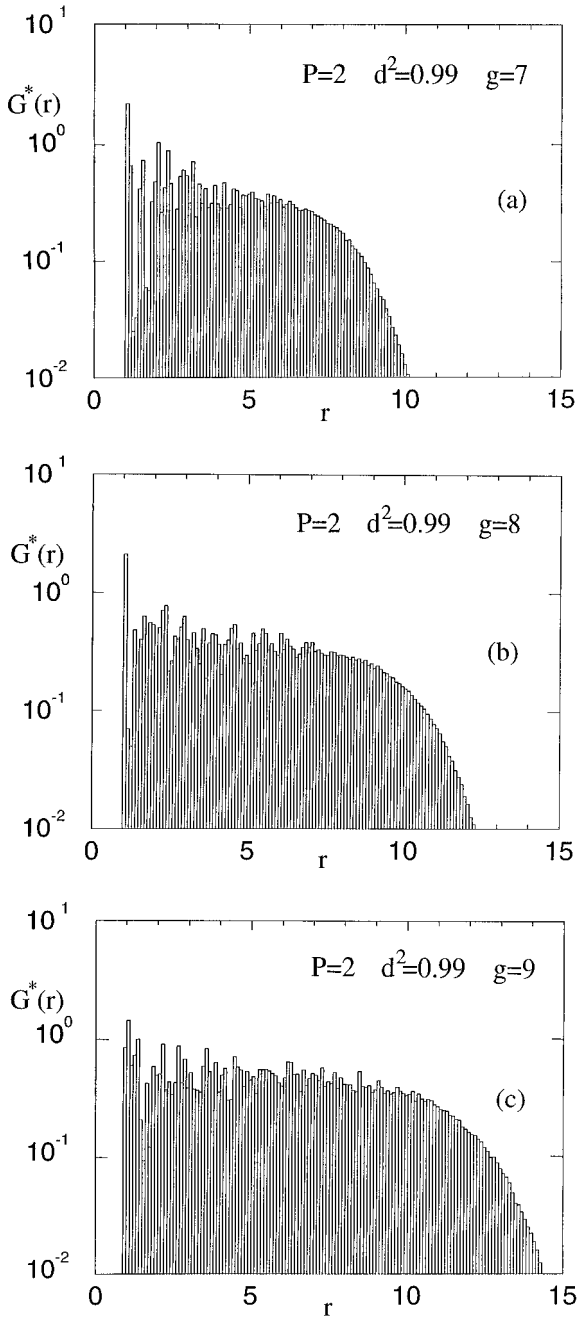

Figure 9. Monomer density as a function of the distance from the center for $P = 2$, $d^2 = 0.99$, and various g as specified in the figures. The strong peaks near $r = 1$ are due to the three beads connected to the center. These systems are in the high volume density regime.

maximum for $G_e(r)$, not for $G(r)$, near the edge of the molecule. The $G_e(r)$ function now exhibits a much stronger maximum peak near the edge compared to the distribution in Figure 3. Both Figures 6 and 7 show that the large-r parts of the distribution functions approach universal limits at large g.

In order to examine the fine structure of the monomer distribution near the central core, we plot in Figures 8 and 9 the rescaled distribution functions for $P = 1$ and $P = 2$ at fixed d^2 (=0.99). There is a strong peak at $r = 0$ (not shown) for each figure, due to the permanent presence of the central bead. The vertical axis is rescaled so that the integrated value $\int_{r_0}^{r_f} G^*(r)4\pi r^2\, dr$ represents the average number of beads appearing in the interval $r = [r_0, r_f]$. The distribution function $G^*(r)$ oscillates near the center. The first strong peak near $r = 1$ is mainly produced by the first three beads connected to the central one. A simple estimate indicates a height of 2.16 for this peak due to the presence of these three beads, which is approximately the height shown in these figures. By using the same reasoning, the peak near $r = 2$ is probably produced by the six beads that are connected to the next generation. Apart from the peaks produced by these central beads, the distribution functions appear to have a weak depletion near the core region in all these figures. The phenomenon was also observed previously by Mansfield and Klushin,[5] who claimed that such a phenomenon is an indication of well-extended central spacers with little folding-back branches, showing the hollow-core behavior predicated

by the stretched-spacer model. Our figures show that the hollowness is very weak, and only exists in the first few generations. Another interesting feature is that when the critical generation is approached, the weak hollow hole begins to disappear, indicating that the branches are forced to fold back because the monomers are making an effort to fill in all available vacancies. For a comparison, the close packing density is approximately $0.74/v$, where $v = (4\pi/3)(d/2)^3 \approx 0.5$, which amounts to about 1.4, almost twice the value of the average density in Figures 8c and 9c.

IV. Summary

We have conducted Monte Carlo simulations to study the scaling behavior of star-burst dendrimers. The scaling function of the mean-square monomer−center distance has been investigated by introducing an excluded-volume parameter z in eq 3. It is remarkable that the conformational properties of molecules that have completely different structures, e.g., branched and linear, can be successfully described by the same scaling exponent. It would be desirable to verify the proposed power law for the radius of gyration in the scaling regime, experimentally or analytically.

Acknowledgment. This work was supported by the Natural Science and Engineering Research Council of Canada.

References and Notes

(1) For a review, see, for example: Fréchet, J. M. *Science* **1994**, *263*, 1710.
(2) de Gennes, P.-G.; Hervet, H. *J. Phys.* (*Paris*) **1983**, *44*, L351.
(3) Lescanec, R. L.; Muthukumar, M. *Macromolecules* **1990**, *23*, 2280.
(4) Mansfield, M. L.; Klushin, L. I. *J. Phys. Chem.* **1992**, *96*, 3994.
(5) Mansfield, M. L.; Klushin, L. I. *Macromolecules* **1993**, *26*, 4262.
(6) Biswas, P.; Cherayil, B. J. *J. Chem. Phys.* **1994**, *100*, 3201.
(7) See, for example: *Monte Carlo and Molecular Dynamic Simulations in Polymer Science*; Binder, K., Ed.; Oxford University Press: New York, 1995.
(8) de Gennes, P.-G. *Scaling Concepts in Polymer Physics*; Cornell University Press: Ithaca, NY, 1979.
(9) Yamakawa, H. *Modern Theory of Polymer Solutions*; Harper and Row: New York, 1971.
(10) Muthukumar, M.; Nickel, B. G. *J. Chem. Phys.* **1987**, *86*, 460.
(11) Zimm, B. H.; Stockmayer, W. *J. Chem. Phys.* **1949**, *17*, 1301.
(12) Flory, P. J. *Principles of Polymer Chemistry*; Cornell University Press: Ithaca, NY, 1953.
(13) Duplantier, B. *J. Stat. Phys.* **1989**, *54*, 581.
(14) Madras, N.; Sokal, A. D. *J. Stat. Phys.* **1988**, *50*, 109.
(15) Barrett, A. J. *J. Phys. A* **1976**, *9*, L33.
(16) Barrett, A. J.; Mansfield, M. L.; Benesch, B. C. *Macromolecules* **1991**, *24*, 1615.
(17) Cui, S.-M.; Chen, Z. Y. *Phys. Rev. B* **1996**, *53*, 6238.
(18) Nickel, B. G. *Macromolecules* **1991**, *24*, 1358.
(19) Chen, Z. Y.; Noolandi, J. *J. Chem. Phys.* **1992**, *96*, 1540.
(20) Miyake, A.; Freed, K. F. *Macromolecules* **1983**, *16*, 1228.
(21) Daoud, M.; Cotton, J. P. *J. Phys.* (*Paris*) **1982**, *43*, 531.
(22) Fisher, M. E. In *Critical Phenomena*; Hahne, F. J. W., Ed.; Lecture Notes in Physics 186; Springer: Berlin, 1982.
(23) *Phase Transitions and Critical Phenomena*; Domb, C., Green, M. S., Eds.; Academic: New York, 1976; Vol. 6.
(24) Chen, Z. Y.; Noolandi, J. *Macromolecules* **1992**, *25*, 4978.

MA9514636